
Graph Attention with Random Rewiring

Tongzhou Liao 

School of Computer Science
Carnegie Mellon University
Pittsburgh, USA

Barnabás Póczos

School of Computer Science
Carnegie Mellon University
Pittsburgh, USA

Abstract

Graph Neural Networks (GNNs) have become fundamental in graph-structured deep learning. Key paradigms of modern GNNs include message passing, graph rewiring, and Graph Transformers. This paper introduces Graph-Rewiring Attention with Stochastic Structures (GRASS), a novel GNN architecture that combines the advantages of these three paradigms. GRASS rewires the input graph by superimposing a random regular graph, enhancing long-range information propagation while preserving structural features of the input graph. It also employs a unique additive attention mechanism tailored for graph-structured data, providing a graph inductive bias while remaining computationally efficient. Our empirical evaluations demonstrate that GRASS achieves state-of-the-art performance on multiple benchmark datasets, confirming its practical efficacy.

1 Introduction

Graph neural networks (GNNs) have emerged as a key innovation in machine learning for tasks involving complex relational data represented as graphs [67, 72]. Central to the advancement of GNNs are message passing neural networks (MPNNs), exemplified by the Graph Convolutional Network (GCN) [39]. By aligning computation with the structure of the graph, MPNNs offer a strong inductive bias for graph-structured data. However, despite recent advances, limitations persist in challenges such as underreaching, which occurs when distant nodes cannot communicate [1], oversmoothing, which occurs when node representations become indistinguishable [52, 15], and oversquashing, which occurs when task-relevant information is excessively compressed [7, 64]. Graph rewiring techniques, aimed at modifying the graph structure to enhance information flow, have shown promise in overcoming these limitations [2]. However, it comes with the risk of distorting the structure of the graph, leading to loss or misinterpretation of relational information [20].

Building GNNs with Transformers [65] presents another promising solution to the above-listed problems. However, many Graph Transformers (GTs) face scalability challenges as a result of their reliance on quadratic-time Transformers [56]. This makes their applicability to large graphs computationally challenging. To address these issues, the General, Powerful, Scalable (GPS) Graph Transformer [56] combines linear-time Transformers with MPNNs to offer a method with $O(|V|+|E|)$ time complexity, where $|V|$ denotes the number of vertices and $|E|$ the number of edges. Exphormer [61], which generalizes sparse Transformers [76] to graphs, represents another promising approach. All these architectures, however, inherit their attention mechanisms from Transformers that are intended for sequences, which are often not optimal for graph-structured data.

Our Contribution. We aim to design a GNN that encompasses the graph inductive bias offered by message passing, the improved information flow achieved through graph rewiring, and the representation power of the attention mechanism. Towards this end, we propose **Graph-Rewiring Attention with Stochastic Structures (GRASS)**, a novel GNN inspired by these three paradigms. GRASS rewires the input graph by superimposing a random regular graph. At each layer, it applies

an attentive node aggregator with attention weights computed from edge representations, and an MLP edge aggregator that updates edge representations to reflect node relationships.

We demonstrate 1) the intuitive and empirical effectiveness of combining random rewiring with message passing, 2) the advantage of a graph-tailored additive attention mechanism over Transformer-style dot-product attention, and 3) the link between randomly rewired message passing and sparse GTs through two interpretations of GRASS. In addition, we show that GRASS achieves state-of-the-art performance on multiple datasets.

In Section 2, we briefly review some related work, highlighting their strengths and weaknesses. In Section 3, we discuss the design principles, architecture, and interpretations of GRASS, our novel GNN. We demonstrate the performance of GRASS in Section 4. We finish the paper with some concluding remarks in Section 5.

2 Related Work

In this section, we briefly summarize some of the prior work related to the main concepts of GRASS.

Graph Rewiring. Graph rewiring involves the strategic modification of graph structures by adding, removing, or reallocating edges. Techniques include deterministic adjustment of the graph structure based on spectral properties [29, 64, 2, 20] and probabilistic rewiring of the graph based on learned distributions [54]. DRew [32] innovatively introduces layer-dependent rewiring, demonstrating outstanding performance on tasks that depend on long-range relationships. While graph rewiring enhances MPNNs by improving graph connectivity, and thus information propagation, they risk compromising informative structural properties of graphs, degrading its inductive bias [20].

Graph Attention and Graph Transformers. Graph Attention Network (GAT) [68] and its successors [9, 78, 70, 11] have leveraged similar attention-based approaches to achieve remarkable results [9, 25]. Despite their success, these MPNNs are intrinsically limited by the structure of the input graph, leading to persistent challenges such as underreaching [1], oversmoothing [52, 15], and oversquashing [7, 64]. At a theoretical level, the expressivity of MPNNs is often no more powerful than the Weisfeiler-Lehman graph isomorphism test [73, 60, 41].

Graph Transformers [75, 22, 40, 74, 48, 36] employ the Transformer architecture [65] to transcend these limitations of MPNNs. Instead of relying on message passing within neighborhoods of the input graph, GTs facilitate simultaneous attention between all nodes, unrestricted by the structure of the graph. However, its $O(|V|^2)$ time complexity becomes prohibitive for large graphs. Linear and sparse Transformers, exemplified by Performer [18] and BigBird [76], respectively, achieve linear runtime with respect to the number of tokens. However, integrating a graph inductive bias into these Transformers can be challenging, since they are designed for Euclidean data [47].

The General, Powerful, Scalable (GPS) Graph Transformer [56] represents a hybrid approach, merging MPNNs’ inductive bias with the global perspective of Linear-Time Transformers. Exphormer [61] presents a natural generalization of BigBird to graphs by incorporating local, global, and random attention. It employs random regular expander graphs as an alternative to BigBird’s random attention patterns on sequential data, and is analogous to the random rewiring mechanism of GRASS. However, these models, along with prior GTs, focus on adapting Transformer-style dot-product attention to graph-structured data, rather than investigating graph-specialized alternatives. Their performance does not exceed that of more tailored attention mechanisms, such as GRIT [47], on a variety of tasks.

Graph Encoding. By integrating structural information directly into nodes and edges, graph encoding significantly improves the expressivity of GNNs, especially for GTs [25]. Techniques such as graph Laplacian positional encoding (LapPE) [25] and random walk structural encoding (RWSE) [23] have been instrumental in this regard. The Graph Inductive Bias Transformer (GRIT) [47] introduces a novel encoding strategy—relative random walk probabilities (RRWP)—which is particularly powerful in capturing structural properties [47]. However, like its GT predecessors, GRIT suffers from $O(|V|^2)$ complexity, limiting its applicability to large graphs.

In summary, while existing methodologies have significantly advanced the field of graph neural networks, they are often constrained by limited expressivity within the MPNN framework, computational inefficiencies, or challenges in incorporating a graph inductive bias. GRASS emerges as a

novel solution that addresses these challenges through the combination of random rewiring and a graph-tailored attention mechanism, offering a competitive solution to graph-structured learning.

3 Methods

In this section, we introduce the design of GRASS. We begin by examining the desirable qualities of a GNN, which guide our architectural design. Subsequently, we introduce the components of GRASS by following the order of data processing in our model, and also describe the role of each component.

Design Goals. We center our design around what we consider to be the key characteristics of an effective GNN. We will focus on the processing of nodes (*N1–N3*) and edges (*E1–E2*), as well as the scalability (*S1*) of the proposed model.

- N1. Permutation Equivariance.* Unlike tokens in a sentence or pixels in an image, nodes in a graph are unordered, and therefore the model should be permutation equivariant by construction. Since reordering the nodes of a graph does not change the graph, permuting the nodes of the input graph of a GNN layer should only result in the same permutation of its output [67]. Formally, let $f(\mathbf{X}, \mathbf{E}, \mathbf{A})$ be the function computed by a layer, where $\mathbf{X} : \mathbb{R}^{|V| \times n_{\text{node}}}$ represents node features with n_{node} dimensions, $\mathbf{E} : \mathbb{R}^{|V| \times |V| \times n_{\text{edge}}}$ represents edge features with n_{edge} dimensions, and $\mathbf{A} : \{0, 1\}^{|V| \times |V|}$ represents the adjacency matrix (edge weights are considered scalar-valued edge features). If the layer is permutation equivariant and $(\mathbf{X}_{\text{out}}, \mathbf{E}_{\text{out}}) = f(\mathbf{X}_{\text{in}}, \mathbf{E}_{\text{in}}, \mathbf{A})$, then $(\mathbf{P}\mathbf{X}_{\text{out}}, \mathbf{P}\mathbf{E}_{\text{out}}\mathbf{P}^\top) = f(\mathbf{P}\mathbf{X}_{\text{in}}, \mathbf{P}\mathbf{E}_{\text{in}}\mathbf{P}^\top, \mathbf{P}\mathbf{A}\mathbf{P}^\top)$ for an arbitrary permutation matrix \mathbf{P} .
- N2. Effective Communication* – The model should facilitate long-range communication between nodes. Numerous real-world tasks require the GNN to capture interactions between distant nodes [24]. However, MPNN layers, which propagate information locally, frequently fail in this regard [47]. A major challenge is underreaching, where an MPNN with l layers is incapable of supporting communication between two nodes x_i, x_j with distance $\delta(x_i, x_j) > l$ [1]. Another challenge is oversquashing, where the structure of the graph forces information from a large set of nodes to squeeze through a small set of nodes to reach its target [64]. A node with a constant-size feature vector may need to relay information from exponentially many nodes (with respect to model depth), leading to excessive compression of messages in deep MPNNs [1]. Addressing these issues is crucial for effectively capturing long-distance relationships.
- N3. Selective Aggregation* – The model should only aggregate information from relevant nodes and edges. MPNN layers commonly update node representations by unconditionally summing or averaging messages from neighboring nodes and edges [67]. In deep models, this can lead to oversmoothing, where the representation of nodes from different classes becomes too similar in the process of repeated aggregation [15]. MPNN like GCN [39] have been shown to behave as low-pass filters in feature vectors [52]. To address this issue, nodes should only aggregate information from relevant neighbors, instead of doing so unconditionally, in order to maintain distinguishability of node representations when required by the task.
- E1. Relationship Representation* – The model should effectively represent the relationships between nodes with edges. Edges in graph-structured data often convey meaningful information about the relationship between the nodes it connects [30]. However, many contemporary GNNs do not use edge features [33, 73, 48], only support scalar-valued edge features (edge weights) [39, 21], or never update edge features across layers [74, 61]. In addition to the semantic relationship represented by edge features of the input graph, structural relationship can be represented by edge encodings added by the model [56]. To inform the model about the relationship between nodes, edge representations should incorporate information from both edge features and edge encodings, and be meaningfully utilized by layers.
- E2. Directionality Preservation* – The model should preserve and utilize information carried by edge directions. Many graphs representing real-world relationships are inherently directed [58]. Although edge directionality has been shown to carry important information for various tasks, many GNN variants require undirected graphs as input, to prevent edge directions from restricting information flow [58]. It would be beneficial for the model’s expressivity if edge directionality information could be preserved without severely limiting communication.
- S1. Efficient Computation* – The model should have $O(|V| + |E|)$ time complexity for its non-precomputable operations. The number of edges $|E|$ in a connected directed graph with $|V|$

vertices may vary from $|V|$ to $|V|(|V| - 1)$. However, in practical scenarios, the number of edges typically falls somewhere between these extremes. GNNs with $O(|V|)$ complexity can be incapable of processing every edge, while those with $O(|V|^2)$ complexity struggle to scale to large-and-sparse graphs where $|E| \in O(|V|)$. Meanwhile, a model with $O(|V| + |E|)$ complexity can be efficient on both dense and sparse graphs. While this is tempting, we notice that computing certain graph properties, such as detecting triangles [71] and finding unweighted all-pair shortest paths [14], cannot be done in $O(|V| + |E|)$ time, which prohibits a model with $O(|V| + |E|)$ time complexity from completing tasks that require these properties. As a compromise, we allow the model to preprocess data without this restriction to capture critical structural properties, as long as the model’s non-precomputable steps remain $O(|V| + |E|)$ time. Precomputable operations only need to be performed once per dataset, regardless of the number of training sessions and epochs, thereby reducing their impact on overall efficiency.

The Structure of GRASS. The high-level structure of GRASS is illustrated in Figure 2. Prior to training, GRASS precomputes the degree matrix and random walk probabilities of each graph in the dataset. At each training iteration, GRASS randomly rewires the input graph, applies node and edge encodings, and passes the graph through multiple attention layers, producing an output graph with the same structure. For tasks that require a graph-level representation, such as graph regression and graph classification, pooling is performed on the output graph to obtain a single output vector.

3.1 Graph Encoding

Extracting structural information plays an important role in graph-structured learning and is crucial for *Relationship Representation*. To this end, GRASS applies relative random walk probabilities (RRWP) encoding [47] and degree encoding [74] to represent structural relationships.

RRWP Encoding. RRWP encoding has been shown to be very expressive both theoretically and practically [47], serving as a major source of structural information for the model. To calculate random walk probabilities, we first obtain the transition matrix \mathbf{T} , where $\mathbf{T}_{i,j}$ represents the probability of moving from node i to node j in a random walk step. It is defined as $\mathbf{T} = \mathbf{D}^{-1}\mathbf{A} : [0, 1]^{|V| \times |V|}$, where $\mathbf{A} \in \{0, 1\}^{|V| \times |V|}$ is the adjacency matrix of the input graph G , and $\mathbf{D} \in \mathbb{N}^{|V| \times |V|}$ is its degree matrix. The powers of \mathbf{T} are stacked to form the RRWP tensor \mathbf{P} , with $\mathbf{P}_{h,i,j}$ representing the probability that a random walker who starts at node i lands at node j at the h -th step. Formally, $\mathbf{P} = [\mathbf{T}, \mathbf{T}^2, \dots, \mathbf{T}^k] : [0, 1]^{k \times |V| \times |V|}$, where k is the number of random walk steps. The diagonal elements $\mathbf{P}_{:,i,i}$ where $i \in V_G$ are used as node encodings, similarly to RWSE [23]. The rest are used as edge encodings when the corresponding edge is present in the rewired graph H . All node encodings undergo Batch Normalization (BN) [37] to improve their distribution, while batch noise also acts as a regularizer that increases the model’s resistance to noise in the random walk probabilities produced by structural noise in the input graph. Here, n denotes the dimensionality of hidden layers.

$$\mathbf{x}_i^{\text{RW}} = \mathbf{W}_{\text{node-enc}} \text{BN}(\mathbf{P}_{:,i,i}) : \mathbb{R}^n \quad (1)$$

$$\mathbf{e}_{i,j}^{\text{RW}} = \mathbf{W}_{\text{edge-enc}} \text{BN}(\mathbf{P}_{:,i,j}) : \mathbb{R}^n \quad (2)$$

As required by *Efficient Computation*, operations slower than $O(|V| + |E|)$ time must be precomputable. \mathbf{P} only needs to be computed once per dataset because it depends only on the adjacency matrix \mathbf{A} of the input graph. To further improve performance through pipelining, the CPU looks up $\mathbf{P}_{:,i,i}$ for each $i \in |V_G|$ and $\mathbf{P}_{:,i,j}$ for each edge $(i, j) \in E_G$ to hide latency and conserve VRAM.

Degree Encoding. Degree encoding is another simple yet powerful way to represent structural information [74]. For datasets in which node degrees can take a small number of values, the model could learn a degree embedding tensor $\mathbf{E} : \mathbb{R}^{D^+ \times D^- \times n}$, where D^+ and D^- denote the maximum out- and in-degree of the dataset, while $d^+(i)$ and $d^-(i)$ represent the out- and in-degree of node i .

$$\mathbf{x}_i^{\text{deg}} = \mathbf{E}_{d^+(i), d^-(i), :} : \mathbb{R}^n \quad (3)$$

For datasets in which degrees can take a large number of values, it could be more efficient to learn degree encodings with a linear layer \mathbf{W}_{deg} , at the cost of expressivity. Here, \parallel denotes concatenation.

$$\mathbf{x}_i^{\text{deg}} = \mathbf{W}_{\text{deg}} \text{BN}(d^+(i) \parallel d^-(i)) : \mathbb{R}^n \quad (4)$$

Applying Encodings. Before entering attention layers, RRWP encodings are added to both node features and edge features (including those of edges added by random rewiring), while degree encodings are only added to node features.

$$\mathbf{x}_i^0 = \mathbf{x}_i^{\text{in}} + \mathbf{x}_i^{\text{RW}} + \mathbf{x}_i^{\text{deg}} : \mathbb{R}^n \quad (5)$$

$$\mathbf{e}_{i,j}^0 = \mathbf{e}_{i,j}^{\text{in}} + \mathbf{e}_{i,j}^{\text{RW}} : \mathbb{R}^n \quad (6)$$

3.2 Random Rewiring

To address the issues of underreaching and oversquashing for *Effective Communication*, GRASS rewires the input graph by superimposing a random regular graph. While deterministic rewiring and non-regular graphs may also improve connectivity, we present potential advantages of using random regular graphs. We also provide details on random regular graph generation and input graph rewiring.

Effects on Diameter. The diameter of a graph upper-bounds the distance between two nodes, and thus the number of layers for an MPNN to propagate information between them [1]. Superimposing a random regular graph onto the input graph can drastically decrease its diameter. The least integer d that satisfies $(r-1)^{d-1} \geq (2+\varepsilon)r|V|\log|V|$ is the upper bound of the diameter of almost every random r -regular graph with $|V|$ nodes, where $r \geq 3$ and $\varepsilon > 0$ [8]. Since adding edges to a graph never increases its diameter, the diameter d of the rewired graph is asymptotically upper-bounded by $d \in O(\log_r |V|)$ when $r \geq 3$. Subsequently, all nodes would be able to communicate with each other given $O(\log_r |V|)$ message passing layers, which could significantly reduce the risk of underreaching on large graphs. In addition, the diameter of a graph is a trivial upper bound of its effective resistance [26], which has been shown to be positively associated with oversquashing [7]. Intuitively, it upper bounds the “length” of the bottleneck through which messages are passed.

Effects on Internally Disjoint Paths. Since oversquashing can be attributed to squeezing too many messages through the fixed-size feature vector of a node [1], increasing the number of internally disjoint paths between two nodes may reduce oversquashing by allowing information to propagate through more nodes in parallel. Intuitively, it increases the “width” of the bottleneck. A random r -regular graph with $r \geq 2$ almost certainly has a vertex connectivity of r as $|V| \rightarrow \infty$ [27]. Menger’s Theorem then lower-bounds the number of internally disjoint paths by a graph’s vertex connectivity [31]. This provides another perspective on how the random regular graph may reduce oversquashing.

Effects on Spectral Gap. Oversquashing has been shown to decrease as the spectral gap of a graph increases, which is defined as λ_1 , the smallest positive eigenvalue of the graph’s Laplacian matrix [38]. It has been proven that a random r -regular graph sampled uniformly from the set of all r -regular graphs with $|V|$ nodes almost certainly has $\mu < 2\sqrt{r-1} + 1$ as $|V| \rightarrow \infty$, where μ is the largest absolute value of nontrivial eigenvalues of its adjacency matrix [53]. Since the graph is r -regular, its i -th adjacency matrix eigenvalue μ_i and i -th Laplacian matrix eigenvalue λ_i satisfy $\lambda_i = r - \mu_i$ [46], lower-bounding the spectral gap with $\lambda_1 > r - 2\sqrt{r-1} - 1$. Therefore, the superimposed random regular graph may alleviate oversquashing by increasing the spectral gap of the rewired graph.

Generating Random Regular Graphs. We generate random regular graphs with the Permutation Model [53] that we describe here and with pseudocode in Appendix A. For a given positive and even parameter $r \geq 2$, and for the input graph $G = (V_G, E_G)$, we randomly generate a corresponding r -regular graph by independently and uniformly sampling $\frac{r}{2}$ random permutations $\sigma_1, \sigma_2, \dots, \sigma_{\frac{r}{2}}$ from $S_{|V_G|}$, the symmetric group defined over the nodes of the graph G . Using these random permutations, we construct a random pseudograph $\tilde{R} = (V_G, E_{\tilde{R}})$, where the edge set $E_{\tilde{R}}$ of the graph \tilde{R} is

$$E_{\tilde{R}} = \bigsqcup_{i \in V_G, j \in [\frac{r}{2}]} \{\{i, \sigma_j(i)\}\} \quad (7)$$

Here, \bigsqcup denotes the disjoint union of sets. The resulting graph \tilde{R} is a random regular pseudograph, and the probability that \tilde{R} is any regular pseudograph with $|V_G|$ nodes and degree r is equal [8]. Being a pseudograph, \tilde{R} might not be simple: it might contain self-loops and multi-edges. Even when $|V_G|$ is large, the probability that \tilde{R} is simple—that it does not contain self-loops or multi-edges—would

not be prohibitively small. In particular, it has an asymptotically tight lower bound [8]:

$$\lim_{|V_G| \rightarrow \infty} \Pr[\tilde{R} \text{ is simple}] = e^{-\frac{r^2}{2} - r} \quad (8)$$

Therefore, if we re-generate \tilde{R} when it's not simple, the expected number of trials required for us to obtain a simple \tilde{R} is upper-bounded by $e^{\frac{r^2}{2} + r}$, which can be kept low by keeping r low. In practice, GRASS would like the superimposed graph to be simple, in order to avoid unwanted redundancy in the attention mechanism. In particular, self-loops result in a duplicate path of message passing from a node to itself, while multi-edges result in multiple identical messages. Meanwhile, the regularity of the graph is desired but not strictly required. Therefore, when \tilde{R} is not simple, we simply remove self-loops and multi-edges from \tilde{R} to obtain R , which is always simple but not necessarily regular.

Rewiring the Input Graph. To rewire the input graph G , GRASS superimposes the edges of R onto G , producing a new graph $H = (V_G, E_G \sqcup E_R)$ that is used as input for subsequent stages of the model. Since it is possible that $E_G \cap E_R \neq \emptyset$, there might be multi-edges in H , and in these cases, H is not a simple graph. GRASS does not remove these multi-edges to avoid biasing the distribution of the superimposed random regular graph.

The added edges E_R are given a distinct embedding to make them distinguishable from the existing edges E_G . This aids *Selective Aggregation*, as it enables a node to select between its neighbors and a random node. Edge encodings are also given to the added edges, which are instrumental in *Relationship Representation*. Although an added edge $(i, j) \in E_R$ lacks edge features that represent semantic relationships in the input graph, the structural relationship between nodes i and j is represented by the random walk probabilities $\mathbf{P}_{:,i,j}$ given to that edge as its RRWP encoding.

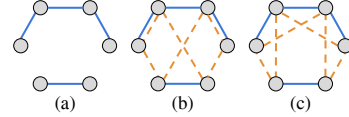


Figure 1: Visualization of the proposed random rewiring mechanism. Solid lines denote existing edges of the input graph, and dashed lines denote added edges. (a) The input graph G . (b, c) Two among all possible instances of the randomly rewired graph H with $r = 2$.

3.3 Attention Mechanism

Many GTs emulate the structure of Transformers designed for Euclidean data [22, 40, 74, 36, 61]. Meanwhile, GRASS uses attentive node aggregators with attention scores computed by MLP edge aggregators, which is a more tailored attention mechanism for graph-structured data. Figure 3 illustrates its structure in detail. The proposed attention mechanism is unique in the way it uses edge representations as the medium of attention weights. To satisfy the needs of *Relationship Representation*, edge representations must be updated alongside node representations. Unlike a node, whose neighborhood is a set of nodes, a directed edge always has one head and one tail which is an ordered pair. An undirected edge can be represented by two directed edges with opposite directions, which allows us to generalize this observation to undirected graphs. With an ordered input, an edge can use an MLP as its aggregator, offering better expressivity by MLP's universal approximation [35] while preserving *Permutation Equivariance*. Assuming *Relationship Representation* is satisfied, edge features would already represent node relationships, which we can use as attention weights $\mathbf{a}_{i,j}$ after applying a linear layer and taking element-wise softmax [10] to obtain a probability distribution.

The proposed attention mechanism is defined as follows, where \odot denotes the Hadamard product, $\hat{\mathbf{d}}^-$ denotes in-degree after random rewiring, and \mathcal{N}^- denotes in-neighbors.

$$\mathbf{s}_{i,j}^l = \text{dropout} \left(\hat{\mathbf{d}}^-(j) \exp(\mathbf{W}_{\text{attn} \leftarrow \text{edge}}^l \mathbf{e}_{i,j}^{l-1}) \right) : \mathbb{R}^{+n} \quad (9)$$

$$\mathbf{a}_{i,j}^l = \frac{\mathbf{s}_{h,j}^l}{\sum_{h \in \mathcal{N}^-(j)} \mathbf{s}_{h,j}^l + \varepsilon} : \mathbb{R}^{+n} \quad (10)$$

$$\tilde{\mathbf{x}}_j^l = \mathbf{W}_{\text{tail} \leftarrow \text{tail}}^l \mathbf{x}_j^{l-1} + \sum_{i \in \mathcal{N}^-(j)} \mathbf{a}_{i,j}^l \odot (\mathbf{W}_{\text{tail} \leftarrow \text{head}}^l \mathbf{x}_i^{l-1} + \mathbf{W}_{\text{tail} \leftarrow \text{edge}}^l \mathbf{e}_{i,j}^{l-1}) : \mathbb{R}^n \quad (11)$$

$$\tilde{\mathbf{e}}_{i,j}^l = \mathbf{W}_{\text{edge} \leftarrow \text{edge}}^l \mathbf{e}_{i,j}^{l-1} + \mathbf{W}_{\text{edge} \leftarrow \text{head}}^l \mathbf{x}_i^{l-1} + \mathbf{W}_{\text{edge} \leftarrow \text{tail}}^l \mathbf{x}_j^{l-1} : \mathbb{R}^n \quad (12)$$

In calculating attention weights, GRASS scales the input to the softmax operation by the logarithm of the number of keys at each node, which is equal to the in-degree of that node after random rewiring.

This has been shown to reduce the impact of the number of keys on the entropy of the distribution of attention weights when there is a large number of keys [17], which supports *Selective Aggregation*. Intuitively, this allows a node to concentrate its attention weight on relevant in-neighbors regardless of the number of in-neighbors it has. Since the number of keys a node attends to is equal to its in-degree, this approach is also analogous to degree scaling [19], which is widely used in MPNNs to incorporate degree information into message passing.

In addition, GRASS uses DropKey [42] as a regularizer, which, in the context of graph attention, is effective in reducing its dependence on the presence of particular edges in the graph. This improves the robustness of GRASS against structural noise and thus facilitates *Selective Aggregation*. DropKey can be seen as the random removal of edges because it randomly masks the attention matrix prior to the softmax operation. Thus, it elegantly complements random rewiring, which only adds edges. This equivalence could not be established for Attention Dropout [77] despite its popularity in Transformers.

Like Transformers, the output of the attention mechanism is passed through an FFN. Here, ϕ denotes a ReLU-like [50, 55, 49] nonlinear activation function.

$$\hat{\mathbf{x}}_i^l = \mathbf{W}_{\text{node-out}}^l \phi(\tilde{\mathbf{x}}_i^l + \mathbf{b}_{\text{node-act}}^l) + \mathbf{b}_{\text{node-out}}^l : \mathbb{R}^n \quad (13)$$

$$\hat{\mathbf{e}}_{j,i}^l = \mathbf{W}_{\text{edge-out}}^l \phi(\tilde{\mathbf{e}}_{i,j}^l + \mathbf{b}_{\text{edge-act}}^l) + \mathbf{b}_{\text{edge-out}}^l : \mathbb{R}^n \quad (14)$$

Normalization and Residual Connection. PN-V is a variant of Power Normalization [59], which normalizes the root mean square of the batch and is more stable than BN on large-variance inputs. BN has been shown to work poorly in GNNs [13], which would be made worse by the variance introduced with random rewiring. PN-V is used by GRASS to address this problem, allowing it to achieve adequate stability during training while still enjoying normalized batch distributions [59].

The residual connection [34] is scaled by α , a coefficient calculated according to DeepNorm [69], which stabilizes the training of deep residual networks. This allows us to use post-normalization, which has been shown to increase expressivity while avoiding the problem of exploding model update [45, 69]. This is essential for us to validate the robustness of GRASS against oversquashing and oversmoothing, which deep GNNs are more vulnerable to, by allowing us to train a deeper model.

$$\mathbf{x}_i^l = \text{PN-V}(\mathbf{x}_i^{l-1} + \alpha \hat{\mathbf{x}}_i^l) : \mathbb{R}^n \quad (15)$$

$$\mathbf{e}_{i,j}^l = \text{PN-V}(\mathbf{e}_{i,j}^{l-1} + \alpha \hat{\mathbf{e}}_{j,i}^l) : \mathbb{R}^n \quad (16)$$

Edge Flipping. While the proposed attention mechanism naturally achieves *Directionality Preservation* by aggregating information in the same direction as edges, it can severely restrict the flow of information, putting it in conflict with *Effective Communication*. As a solution, the direction of each edge is switched from one layer to the next: in odd-numbered layers, the directions match those of the edges in the rewired graph H , whereas in even-numbered layers, they are reversed. This enables the model to propagate information in both directions even when the input graph is directed, improving its expressivity [58]. We empirically find edge flipping to be beneficial on undirected graphs (where an undirected edge is represented as a pair of directed edges with opposite directions) as well.

Graph Pooling. For graph-level tasks, graph pooling is required at the output of a GNN to produce a vector representation of each graph, capturing task-relevant global properties [72]. GRASS employs sum pooling, a simple pooling method as powerful as the Weisfeiler-Lehman test, while many more complicated methods are not [4]. Considering the randomness of the added edges, they are pooled separately from the preexisting edges in the input graph G , because the pooled output of the randomly added edges may exhibit a different distribution than that of the preexisting edges. Here, \parallel denotes concatenation.

$$\mathbf{y} = \sum_{i \in V_G} \mathbf{x}_i^L \parallel \left\| \sum_{(i,j) \in E_G} \mathbf{e}_{i,j}^L \right\| \parallel \sum_{(i,j) \in E_R} \mathbf{e}_{i,j}^L : \mathbb{R}^{3n} \quad (17)$$

3.4 Interpretations of GRASS

A Message Passing Perspective. GRASS is an MPNN on a noisy graph. In an MPNN, information is propagated along the edges of the input graph, defined by its adjacency matrix [67]. GRASS can be seen as an MPNN that injects additive and multiplicative noise into the adjacency matrix, through

random rewiring and DropKey, respectively. The adjacency matrix \mathbf{A}_M followed by message passing is given by

$$\mathbf{A}_M = (\mathbf{A}_G + \mathbf{A}_R) \cdot \mathbf{A}_D \quad (18)$$

where \mathbf{A}_G is the adjacency matrix of the input graph G , \mathbf{A}_R is that of the superimposed random regular graph R , \mathbf{A}_D is a random attention mask sampled by DropKey (which can also be seen as the adjacency matrix of a random graph), $+$ denotes element-wise OR, and \cdot denotes element-wise AND.

Noise injection is well known as an effective regularizer [51], and for graph-structured data, the random removal of edges has demonstrated regularization effects [57]. By adding noise to the adjacency matrix that guides the propagation of information in message passing, GRASS is encouraged to develop robustness against structural noise, which is prevalent in graph-structured data [66].

A Graph Transformer Perspective. GRASS is a sparse Graph Transformer. Graph Transformers allow each node to aggregate information from other nodes through graph attention mechanisms, with a general definition [67] being

$$\mathbf{x}'_j = \phi \left(\mathbf{x}_j, \bigoplus_{i \in \mathcal{N}(j)} a(\mathbf{x}_i, \mathbf{x}_j) \psi(\mathbf{x}_i) \right) \quad (19)$$

where ϕ and ψ are neural networks, a is an attention weight function, and \bigoplus is a permutation-invariant aggregator. Many GTs compute attention weights using scaled dot-product attention [65], with node features as keys and queries. However, we observe that edge features in GRASS, which are updated by aggregating information from its head and tail nodes with an MLP, could be used to directly compute attention weights as a form of additive attention [5]. *Relationship Representation* would then be critical for the attention weights to be meaningful, which GRASS satisfies through expressive edge encodings and the deep processing of edge features.

Many GTs achieve sparsity by integrating [56] or generalizing [61] BigBird’s sparse dot-product attention. Meanwhile, GRASS achieves sparsity in a graph-native way: attention is always local, so nonadjacent nodes in the rewired graph would naturally never attend to each other. Seeing GRASS as a Transformer, its attention mask would be \mathbf{A}_M as defined in Equation 18. Moreover, there might be little computational benefit in using sparse dot-product attention on graphs-structured data, since its efficient implementation relies on efficient sparse matrix multiplication [76], which is challenging [28, 12] due to the lack of exploitable sparsity patterns in many real-world graphs.

4 Experiments

Benchmarking GRASS. To measure the performance of GRASS, we train and evaluate it on five of the GNN Benchmark Datasets [25]: ZINC, MNIST, CIFAR10, CLUSTER, and PATTERN, as well as three of the Long Range Graph Benchmark (LRGB) [24] datasets: Peptides-func, Peptides-struct, and PascalVOC-SP. Following the experimental setup of Rampášek et al. [56], we configure GRASS to around 100k parameters for MNIST and CIFAR10, and 500k parameters for all other datasets. Additional information on the datasets can be found in Appendix D. In all experiments, we use the Lion optimizer [16] and the 1cycle learning rate schedule [62].

As shown in Tables 1 and 2, GRASS ranks first in ZINC, MNIST, CIFAR, PATTERN, Peptides-struct, and PascalVOC-SP, while ranking second in CLUSTER. Notably, GRASS achieves 21.9% lower MAE in ZINC compared to GRIT, the second-best model on the dataset, which has $O(|V|^2)$ runtime.

It has been suggested that oversmoothing can be alleviated by having a shallow GNN, and oversquashing can be avoided by having wide hidden layers [64]. However, narrow-and-deep GNNs can have better expressivity than wide-and-shallow GNNs if the pitfalls of training deep GNNs, such as oversmoothing and oversquashing, can be avoided [43, 44]. This could potentially explain the competitive performance of GRASS which we configured to be narrow and deep in our experiments, as specified in Appendix E. In addition, the datasets we tested are relatively small in sample size (<100k samples), which makes a good inductive bias more important [6, 47], highlighting the ability of GRASS to provide a strong inductive bias on graph-structured data while remaining computationally efficient.

Ablation Study. GRASS achieves its design goals with multiple components, whose importance is evaluated in the ablation studies shown in Table 3. In particular, the performance of GRASS with different values of r , the degree of the superimposed random regular graph, is compared in Table 4.

Table 1: Performance on GNN Benchmark Datasets. The performance of GRASS shown here is the mean \pm s.d. of 8 runs on ZINC, and 6 runs on other datasets. The **best** and **second-best** results are highlighted. Performance numbers other than that of GRASS are adapted from Ma et al. [47] and Shirzad et al. [61].

Model	ZINC	MNIST	CIFAR10	PATTERN	CLUSTER
	MAE \downarrow	Accuracy \uparrow	Accuracy \uparrow	Accuracy \uparrow	Accuracy \uparrow
GCN	0.367 \pm 0.011	90.705 \pm 0.218	55.710 \pm 0.381	71.892 \pm 0.334	68.498 \pm 0.976
GIN	0.526 \pm 0.051	96.485 \pm 0.252	55.255 \pm 1.527	85.387 \pm 0.136	64.716 \pm 1.553
GAT	0.384 \pm 0.007	95.535 \pm 0.205	64.223 \pm 0.455	78.271 \pm 0.186	70.587 \pm 0.447
GatedGCN	0.282 \pm 0.015	97.340 \pm 0.143	67.312 \pm 0.311	85.568 \pm 0.088	73.840 \pm 0.326
GatedGCN-LSPE	0.090 \pm 0.001	-	-	-	-
PNA	0.188 \pm 0.004	97.94 \pm 0.12	70.35 \pm 0.63	-	-
DGN	0.168 \pm 0.003	-	72.838 \pm 0.417	86.680 \pm 0.034	-
GSN	0.101 \pm 0.010	-	-	-	-
CIN	0.079 \pm 0.006	-	-	-	-
CRaW1	0.085 \pm 0.004	97.944 \pm 0.050	69.013 \pm 0.259	-	-
GIN-AK+	0.080 \pm 0.001	-	72.19 \pm 0.13	86.850 \pm 0.057	-
SAN	0.139 \pm 0.006	-	-	-	76.691 \pm 0.65
Graphormer	0.122 \pm 0.006	-	-	-	-
K-Subgraph SAT	0.094 \pm 0.008	-	-	86.848 \pm 0.037	77.856 \pm 0.104
EGT	0.108 \pm 0.009	98.173 \pm 0.087	68.702 \pm 0.409	86.821 \pm 0.020	79.232 \pm 0.348
Graphormer-URPE	0.086 \pm 0.007	-	-	-	-
Graphormer-GD	0.081 \pm 0.009	-	-	-	-
GPS	0.070 \pm 0.004	-	72.298 \pm 0.356	86.685 \pm 0.059	78.016 \pm 0.180
Expormer	-	98.55 \pm 0.039	74.69 \pm 0.125	86.74 \pm 0.015	78.07 \pm 0.037
GRIT	0.059 \pm 0.002	98.108 \pm 0.111	76.468 \pm 0.881	87.196 \pm 0.076	80.026 \pm 0.277
GRASS (ours)	0.046 \pm 0.001	98.905 \pm 0.034	82.471 \pm 0.319	90.997 \pm 0.225	79.347 \pm 0.087

Table 2: Performance on LRGB datasets. The performance of GRASS shown here is the mean \pm s.d. of 8 runs. The **best** and **second-best** results are highlighted. Performance numbers other than that of GRASS are adapted from Gutteridge et al. [32], Tönshoff et al. [63], Ma et al. [47], and Shirzad et al. [61]. *Tönshoff et al. [63] has improved the performance of these models via hyperparameter tuning.

Model	Peptides-func	Peptides-struct	PascalVOC-SP
	AP \uparrow	MAE \downarrow	Macro F1 \uparrow
GCN*	0.6860 \pm 0.0050	0.2460 \pm 0.0007	0.2078 \pm 0.0031
GINE*	0.6621 \pm 0.0067	0.2473 \pm 0.0017	0.2718 \pm 0.0054
GatedGCN*	0.6765 \pm 0.0047	0.2477 \pm 0.0009	0.3880 \pm 0.0040
DIGL+MPNN	0.6469 \pm 0.0019	0.3173 \pm 0.0007	0.2824 \pm 0.0039
DIGL+MPNN+LapPE	0.6830 \pm 0.0026	0.2616 \pm 0.0018	0.2921 \pm 0.0038
MixHop-GCN	0.6592 \pm 0.0036	0.2921 \pm 0.0023	0.2506 \pm 0.0133
MixHop-GCN+LapPE	0.6843 \pm 0.0049	0.2614 \pm 0.0023	0.2218 \pm 0.0174
DRew-GCN	0.6996 \pm 0.0076	0.2781 \pm 0.0028	0.1848 \pm 0.0107
DRew-GCN+LapPE	0.7150 \pm 0.0044	0.2536 \pm 0.0015	0.1851 \pm 0.0092
DRew-GIN	0.6940 \pm 0.0074	0.2799 \pm 0.0016	0.2719 \pm 0.0043
DRew-GIN+LapPE	0.7126 \pm 0.0045	0.2606 \pm 0.0014	0.2692 \pm 0.0059
DRew-GatedGCN	0.6733 \pm 0.0094	0.2699 \pm 0.0018	0.3214 \pm 0.0021
DRew-GatedGCN+LapPE	0.6977 \pm 0.0026	0.2539 \pm 0.0007	0.3314 \pm 0.0024
Transformer+LapPE	0.6326 \pm 0.0126	0.2529 \pm 0.0016	0.2694 \pm 0.0098
SAN+LapPE	0.6384 \pm 0.0121	0.2683 \pm 0.0043	0.3230 \pm 0.0039
GPS+LapPE*	0.6534 \pm 0.0091	0.2509 \pm 0.0014	0.4440 \pm 0.0065
Expormer	0.6527 \pm 0.0043	0.2481 \pm 0.0007	0.3975 \pm 0.0037
GRIT	0.6988 \pm 0.0082	0.2460 \pm 0.0012	-
GRASS (ours)	0.6353 \pm 0.0056	0.2447 \pm 0.0009	0.5633 \pm 0.0092

5 Conclusion

GRASS demonstrates the effectiveness of random rewiring and our graph-tailored attention mechanism by achieving state-of-the-art performance, surpassing more elaborate methods of graph rewiring, as well as more computationally demanding Graph Transformers. To improve the reproducibility of our results, our codebase will be made publicly available on GitHub.

Limitations. The output of GRASS is inherently random due to random rewiring. The relationship between performance variance and r is demonstrated in Table 4. In scenarios that strictly require deterministic model output, the random number generator used for random rewiring should be seeded with the input graph, making the deployment of GRASS more complicated in these scenarios.

References

- [1] Uri Alon and Eran Yahav. On the bottleneck of graph neural networks and its practical implications. *arXiv preprint arXiv:2006.05205*, 2020.
- [2] Adrian Arnaiz-Rodriguez, Ahmed Begga, Francisco Escolano, and Nuria Oliver. Diffwire: Inductive graph rewiring via the lovasz bound. In *The First Learning on Graphs Conference*, 2022.
- [3] Jimmy Lei Ba, Jamie Ryan Kiros, and Geoffrey E Hinton. Layer normalization. *arXiv preprint arXiv:1607.06450*, 2016.
- [4] Jinheon Baek, Minki Kang, and Sung Ju Hwang. Accurate learning of graph representations with graph multiset pooling. *arXiv preprint arXiv:2102.11533*, 2021.
- [5] Dzmitry Bahdanau, Kyunghyun Cho, and Yoshua Bengio. Neural machine translation by jointly learning to align and translate. *arXiv preprint arXiv:1409.0473*, 2014.
- [6] Jonathan Baxter. A model of inductive bias learning. *Journal of artificial intelligence research*, 12:149–198, 2000.
- [7] Mitchell Black, Zhengchao Wan, Amir Nayyeri, and Yusu Wang. Understanding oversquashing in gnns through the lens of effective resistance. In *International Conference on Machine Learning*, pages 2528–2547. PMLR, 2023.
- [8] Béla Bollobás and W Fernandez de la Vega. The diameter of random regular graphs. *Combinatorica*, 2:125–134, 1982.
- [9] Xavier Bresson and Thomas Laurent. Residual gated graph convnets. *arXiv preprint arXiv:1711.07553*, 2017.
- [10] John S Bridle. Probabilistic interpretation of feedforward classification network outputs, with relationships to statistical pattern recognition. In *Neurocomputing: Algorithms, architectures and applications*, pages 227–236. Springer, 1990.
- [11] Shaked Brody, Uri Alon, and Eran Yahav. How attentive are graph attention networks? *arXiv preprint arXiv:2105.14491*, 2021.
- [12] Aydin Buluc and John R Gilbert. Challenges and advances in parallel sparse matrix-matrix multiplication. In *2008 37th International Conference on Parallel Processing*, pages 503–510. IEEE, 2008.
- [13] Tianle Cai, Shengjie Luo, Keyulu Xu, Di He, Tie-yan Liu, and Liwei Wang. Graphnorm: A principled approach to accelerating graph neural network training. In *International Conference on Machine Learning*, pages 1204–1215. PMLR, 2021.
- [14] Timothy M Chan, Virginia Vassilevska Williams, and Yinzhan Xu. Fredman’s trick meets dominance product: Fine-grained complexity of unweighted apsp, 3sum counting, and more. In *Proceedings of the 55th Annual ACM Symposium on Theory of Computing*, pages 419–432, 2023.
- [15] Deli Chen, Yankai Lin, Wei Li, Peng Li, Jie Zhou, and Xu Sun. Measuring and relieving the over-smoothing problem for graph neural networks from the topological view. In *Proceedings of the AAAI conference on artificial intelligence*, volume 34, pages 3438–3445, 2020.
- [16] Xiangning Chen, Chen Liang, Da Huang, Esteban Real, Kaiyuan Wang, Yao Liu, Hieu Pham, Xuanyi Dong, Thang Luong, Cho-Jui Hsieh, et al. Symbolic discovery of optimization algorithms. *arXiv preprint arXiv:2302.06675*, 2023.
- [17] David Chiang and Peter Cholak. Overcoming a theoretical limitation of self-attention. *arXiv preprint arXiv:2202.12172*, 2022.
- [18] Krzysztof Choromanski, Valerii Likhoshesterov, David Dohan, Xingyou Song, Andreea Gane, Tamas Sarlos, Peter Hawkins, Jared Davis, Afroz Mohiuddin, Lukasz Kaiser, et al. Rethinking attention with performers. *arXiv preprint arXiv:2009.14794*, 2020.

- [19] Gabriele Corso, Luca Cavalleri, Dominique Beaini, Pietro Liò, and Petar Veličković. Principal neighbourhood aggregation for graph nets. *Advances in Neural Information Processing Systems*, 33:13260–13271, 2020.
- [20] Andreea Deac, Marc Lackenby, and Petar Veličković. Expander graph propagation. In *Learning on Graphs Conference*, pages 38–1. PMLR, 2022.
- [21] Michaël Defferrard, Xavier Bresson, and Pierre Vandergheynst. Convolutional neural networks on graphs with fast localized spectral filtering. *Advances in neural information processing systems*, 29, 2016.
- [22] Vijay Prakash Dwivedi and Xavier Bresson. A generalization of transformer networks to graphs. *arXiv preprint arXiv:2012.09699*, 2020.
- [23] Vijay Prakash Dwivedi, Anh Tuan Luu, Thomas Laurent, Yoshua Bengio, and Xavier Bresson. Graph neural networks with learnable structural and positional representations. *arXiv preprint arXiv:2110.07875*, 2021.
- [24] Vijay Prakash Dwivedi, Ladislav Rampásek, Michael Galkin, Ali Parviz, Guy Wolf, Anh Tuan Luu, and Dominique Beaini. Long range graph benchmark. *Advances in Neural Information Processing Systems*, 35:22326–22340, 2022.
- [25] Vijay Prakash Dwivedi, Chaitanya K Joshi, Anh Tuan Luu, Thomas Laurent, Yoshua Bengio, and Xavier Bresson. Benchmarking graph neural networks. *Journal of Machine Learning Research*, 24(43):1–48, 2023.
- [26] Wendy Ellens, Floske M Spijksma, Piet Van Mieghem, Almerima Jamakovic, and Robert E Kooij. Effective graph resistance. *Linear algebra and its applications*, 435(10):2491–2506, 2011.
- [27] David Ellis. The expansion of random regular graphs. *Lecture Notes, Lent*, 34, 2011.
- [28] Jianhua Gao, Weixing Ji, Fangli Chang, Shiyu Han, Bingxin Wei, Zeming Liu, and Yizhuo Wang. A systematic survey of general sparse matrix-matrix multiplication. *ACM Computing Surveys*, 55(12):1–36, 2023.
- [29] Johannes Gasteiger, Stefan Weißenberger, and Stephan Günnemann. Diffusion improves graph learning. *Advances in neural information processing systems*, 32, 2019.
- [30] Liyu Gong and Qiang Cheng. Exploiting edge features for graph neural networks. In *Proceedings of the IEEE/CVF conference on computer vision and pattern recognition*, pages 9211–9219, 2019.
- [31] Frank Göring. Short proof of menger’s theorem. *Discrete Mathematics*, 219(1-3):295–296, 2000.
- [32] Benjamin Gutteridge, Xiaowen Dong, Michael M Bronstein, and Francesco Di Giovanni. Drew: Dynamically rewired message passing with delay. In *International Conference on Machine Learning*, pages 12252–12267. PMLR, 2023.
- [33] Will Hamilton, Zhitao Ying, and Jure Leskovec. Inductive representation learning on large graphs. *Advances in neural information processing systems*, 30, 2017.
- [34] Kaiming He, Xiangyu Zhang, Shaoqing Ren, and Jian Sun. Deep residual learning for image recognition. In *Proceedings of the IEEE conference on computer vision and pattern recognition*, pages 770–778, 2016.
- [35] Kurt Hornik, Maxwell Stinchcombe, and Halbert White. Multilayer feedforward networks are universal approximators. *Neural networks*, 2(5):359–366, 1989.
- [36] Md Shamim Hussain, Mohammed J Zaki, and Dharmashankar Subramanian. Global self-attention as a replacement for graph convolution. In *Proceedings of the 28th ACM SIGKDD Conference on Knowledge Discovery and Data Mining*, pages 655–665, 2022.

- [37] Sergey Ioffe and Christian Szegedy. Batch normalization: Accelerating deep network training by reducing internal covariate shift. In *International conference on machine learning*, pages 448–456. pmlr, 2015.
- [38] Kedar Karhadkar, Pradeep Kr Banerjee, and Guido Montúfar. Fcsr: First-order spectral rewiring for addressing oversquashing in gnns. *arXiv preprint arXiv:2210.11790*, 2022.
- [39] Thomas N Kipf and Max Welling. Semi-supervised classification with graph convolutional networks. *arXiv preprint arXiv:1609.02907*, 2016.
- [40] Devin Kreuzer, Dominique Beaini, Will Hamilton, Vincent Létourneau, and Prudencio Tossou. Rethinking graph transformers with spectral attention. *Advances in Neural Information Processing Systems*, 34:21618–21629, 2021.
- [41] AA Leman and Boris Weisfeiler. A reduction of a graph to a canonical form and an algebra arising during this reduction. *Nauchno-Tekhnicheskaya Informatsiya*, 2(9):12–16, 1968.
- [42] Bonan Li, Yinhan Hu, Xuecheng Nie, Congying Han, Xiangjian Jiang, Tiande Guo, and Luoqi Liu. Dropkey. *arXiv preprint arXiv:2208.02646*, 2022.
- [43] Guohao Li, Chenxin Xiong, Ali Thabet, and Bernard Ghanem. Deepergcn: All you need to train deeper gcns. *arXiv preprint arXiv:2006.07739*, 2020.
- [44] Guohao Li, Matthias Müller, Bernard Ghanem, and Vladlen Koltun. Training graph neural networks with 1000 layers. In *International conference on machine learning*, pages 6437–6449. PMLR, 2021.
- [45] Liyuan Liu, Xiaodong Liu, Jianfeng Gao, Weizhu Chen, and Jiawei Han. Understanding the difficulty of training transformers. *arXiv preprint arXiv:2004.08249*, 2020.
- [46] JF Lutzeyer and AT Walden. Comparing graph spectra of adjacency and laplacian matrices. *arXiv preprint arXiv:1712.03769*, 2017.
- [47] Liheng Ma, Chen Lin, Derek Lim, Adriana Romero-Soriano, Puneet K Dokania, Mark Coates, Philip Torr, and Ser-Nam Lim. Graph inductive biases in transformers without message passing. *arXiv preprint arXiv:2305.17589*, 2023.
- [48] Grégoire Mialon, Dexiong Chen, Margot Selosse, and Julien Mairal. Graphit: Encoding graph structure in transformers. *arXiv preprint arXiv:2106.05667*, 2021.
- [49] Diganta Misra. Mish: A self regularized non-monotonic activation function. *arXiv preprint arXiv:1908.08681*, 2019.
- [50] Vinod Nair and Geoffrey E Hinton. Rectified linear units improve restricted boltzmann machines. In *Proceedings of the 27th international conference on machine learning (ICML-10)*, pages 807–814, 2010.
- [51] Hyeonwoo Noh, Tackgeun You, Jonghwan Mun, and Bohyung Han. Regularizing deep neural networks by noise: Its interpretation and optimization. *Advances in neural information processing systems*, 30, 2017.
- [52] Hoang Nt and Takanori Maehara. Revisiting graph neural networks: All we have is low-pass filters. *arXiv preprint arXiv:1905.09550*, 2019.
- [53] Doron Puder. Expansion of random graphs: New proofs, new results. *Inventiones mathematicae*, 201(3):845–908, 2015.
- [54] Chendi Qian, Andrei Manolache, Kareem Ahmed, Zhe Zeng, Guy Van den Broeck, Mathias Niepert, and Christopher Morris. Probabilistically rewired message-passing neural networks. *arXiv preprint arXiv:2310.02156*, 2023.
- [55] Prajit Ramachandran, Barret Zoph, and Quoc V Le. Searching for activation functions. *arXiv preprint arXiv:1710.05941*, 2017.

- [56] Ladislav Rampásek, Michael Galkin, Vijay Prakash Dwivedi, Anh Tuan Luu, Guy Wolf, and Dominique Beaini. Recipe for a general, powerful, scalable graph transformer. *Advances in Neural Information Processing Systems*, 35:14501–14515, 2022.
- [57] Yu Rong, Wenbing Huang, Tingyang Xu, and Junzhou Huang. Dropedge: Towards deep graph convolutional networks on node classification. *arXiv preprint arXiv:1907.10903*, 2019.
- [58] Emanuele Rossi, Bertrand Charpentier, Francesco Di Giovanni, Fabrizio Frasca, Stephan Günnemann, and Michael M Bronstein. Edge directionality improves learning on heterophilic graphs. In *Learning on Graphs Conference*, pages 25–1. PMLR, 2024.
- [59] Sheng Shen, Zhewei Yao, Amir Gholami, Michael Mahoney, and Kurt Keutzer. Powernorm: Rethinking batch normalization in transformers. In *International Conference on Machine Learning*, pages 8741–8751. PMLR, 2020.
- [60] Nino Shervashidze, Pascal Schweitzer, Erik Jan Van Leeuwen, Kurt Mehlhorn, and Karsten M Borgwardt. Weisfeiler-lehman graph kernels. *Journal of Machine Learning Research*, 12(9), 2011.
- [61] Hamed Shirzad, Ameya Velingker, Balaji Venkatachalam, Danica J Sutherland, and Ali Kemal Sinop. Exphormer: Sparse transformers for graphs. In *International Conference on Machine Learning*, pages 31613–31632. PMLR, 2023.
- [62] Leslie N Smith and Nicholay Topin. Super-convergence: Very fast training of neural networks using large learning rates. In *Artificial intelligence and machine learning for multi-domain operations applications*, volume 11006, pages 369–386. SPIE, 2019.
- [63] Jan Tönshoff, Martin Ritzert, Eran Rosenbluth, and Martin Grohe. Where did the gap go? reassessing the long-range graph benchmark. *arXiv preprint arXiv:2309.00367*, 2023.
- [64] Jake Topping, Francesco Di Giovanni, Benjamin Paul Chamberlain, Xiaowen Dong, and Michael M Bronstein. Understanding over-squashing and bottlenecks on graphs via curvature. *arXiv preprint arXiv:2111.14522*, 2021.
- [65] Ashish Vaswani, Noam Shazeer, Niki Parmar, Jakob Uszkoreit, Llion Jones, Aidan N Gomez, Łukasz Kaiser, and Illia Polosukhin. Attention is all you need. *Advances in neural information processing systems*, 30, 2017.
- [66] Petar Veličković. Message passing all the way up. *arXiv preprint arXiv:2202.11097*, 2022.
- [67] Petar Veličković. Everything is connected: Graph neural networks. *Current Opinion in Structural Biology*, 79:102538, 2023.
- [68] Petar Veličković, Guillem Cucurull, Arantxa Casanova, Adriana Romero, Pietro Lio, and Yoshua Bengio. Graph attention networks. *arXiv preprint arXiv:1710.10903*, 2017.
- [69] Hongyu Wang, Shuming Ma, Li Dong, Shaohan Huang, Dongdong Zhang, and Furu Wei. Deepnet: Scaling transformers to 1,000 layers. *arXiv preprint arXiv:2203.00555*, 2022.
- [70] Xiao Wang, Houye Ji, Chuan Shi, Bai Wang, Yanfang Ye, Peng Cui, and Philip S Yu. Heterogeneous graph attention network. In *The world wide web conference*, pages 2022–2032, 2019.
- [71] Virginia Vassilevska Williams and Ryan Williams. Triangle detection versus matrix multiplication: A study of truly subcubic reducibility. 2009.
- [72] Zonghan Wu, Shirui Pan, Fengwen Chen, Guodong Long, Chengqi Zhang, and S Yu Philip. A comprehensive survey on graph neural networks. *IEEE transactions on neural networks and learning systems*, 32(1):4–24, 2020.
- [73] Keyulu Xu, Weihua Hu, Jure Leskovec, and Stefanie Jegelka. How powerful are graph neural networks? *arXiv preprint arXiv:1810.00826*, 2018.

- [74] Chengxuan Ying, Tianle Cai, Shengjie Luo, Shuxin Zheng, Guolin Ke, Di He, Yanming Shen, and Tie-Yan Liu. Do transformers really perform badly for graph representation? *Advances in Neural Information Processing Systems*, 34:28877–28888, 2021.
- [75] Seongjun Yun, Minbyul Jeong, Raehyun Kim, Jaewoo Kang, and Hyunwoo J Kim. Graph transformer networks. *Advances in neural information processing systems*, 32, 2019.
- [76] Manzil Zaheer, Guru Guruganesh, Kumar Avinava Dubey, Joshua Ainslie, Chris Alberti, Santiago Ontanon, Philip Pham, Anirudh Ravula, Qifan Wang, Li Yang, et al. Big bird: Transformers for longer sequences. *Advances in neural information processing systems*, 33: 17283–17297, 2020.
- [77] Lin Zehui, Pengfei Liu, Luyao Huang, Junkun Chen, Xipeng Qiu, and Xuanjing Huang. Dropattention: A regularization method for fully-connected self-attention networks. *arXiv preprint arXiv:1907.11065*, 2019.
- [78] Jiani Zhang, Xingjian Shi, Junyuan Xie, Hao Ma, Irwin King, and Dit-Yan Yeung. Gaan: Gated attention networks for learning on large and spatiotemporal graphs. *arXiv preprint arXiv:1803.07294*, 2018.

A Pseudocode of the Permutation Model

Algorithm 1 The Permutation Model

```

1: procedure PERMUTATIONMODEL( $r, |V|$ )
2:    $\sigma \leftarrow$  2D array of size  $(r, |V|)$ 
3:   for  $i \leftarrow 0$  to  $r - 1$  do
4:      $\sigma[i, :] \leftarrow$  RANDPERM( $|V|$ )  $\triangleright$  Random permutation of integers between 0 and  $|V| - 1$ 
5:   end for
6:    $A \leftarrow$  Array of size  $r \times |V|$   $\triangleright$  Create an empty adjacency list
7:   for  $j \leftarrow 0$  to  $|V|$  do
8:     for  $k \leftarrow 0$  to  $r$  do
9:        $A[j \times r + k] \leftarrow \{j, \sigma[k, j]\}$   $\triangleright$  Add an edge to the adjacency list
10:    end for
11:  end for
12:   $A \leftarrow$  REMOVESELFLOOP( $A$ )  $\triangleright$  Remove self-loops from the adjacency list
13:   $A \leftarrow$  REMOVMULTIEDGE( $A$ )  $\triangleright$  Remove multi-edges from the adjacency list
14:  return  $A$ 
15: end procedure

```

B Graphical Descriptions of GRASS

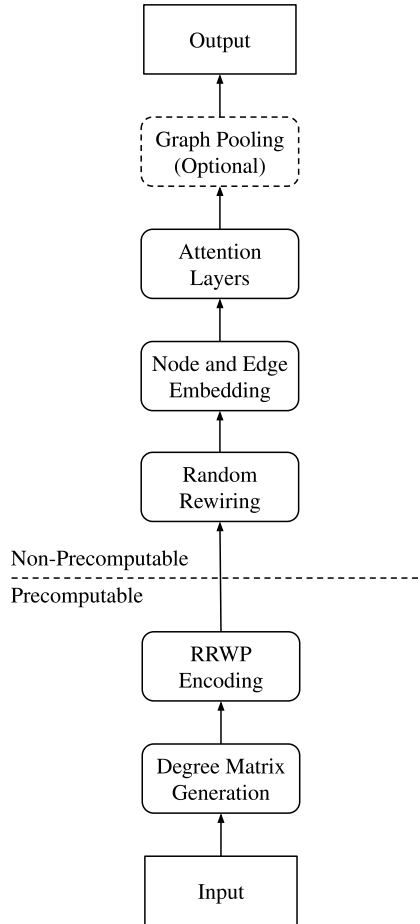


Figure 2: The high-level structure of GRASS.

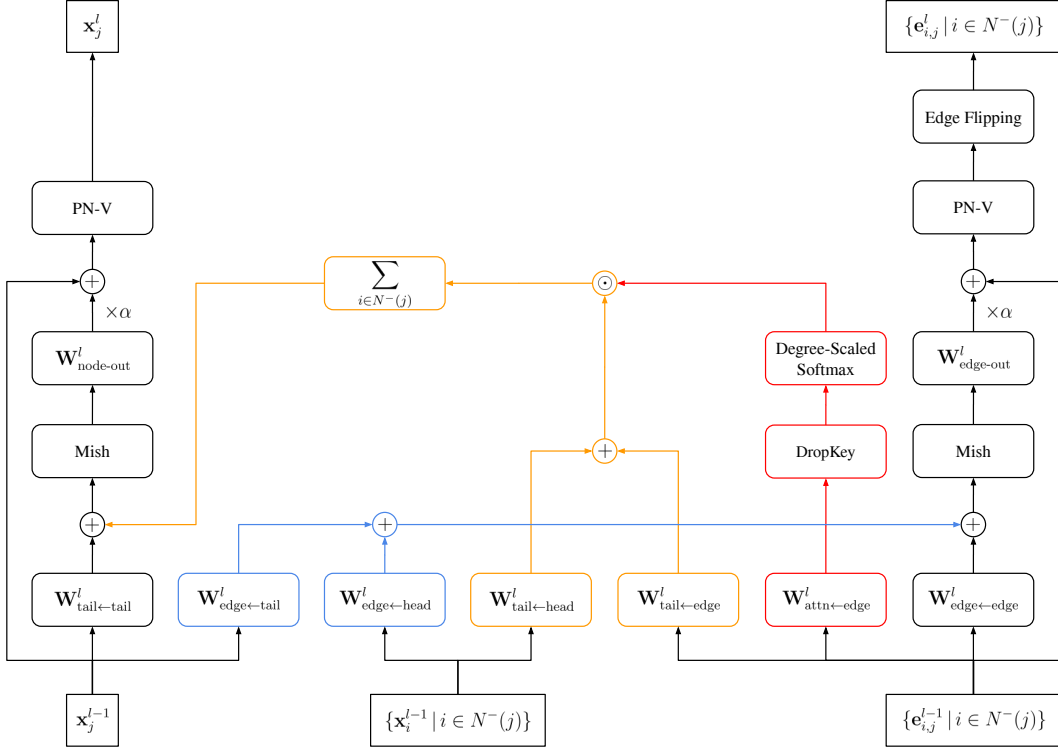


Figure 3: The structure of an attention layer of GRASS. **Node aggregation** is attentive, with **attention weights** derived from edge representations. **Edge aggregation** is done through an FFN. For simplicity, biases are not shown here.

C Ablation Study

Table 3: Ablation study results on different components of GRASS. This table shows the performance of each ablated model as the mean \pm s.d. over 8 runs. *The absolute difference between the LapPEs (8 eigenvalues) of neighboring nodes are used as edge encodings, as proposed by Kreuzer et al. [40].

Model	ZINC MAE \downarrow
GRASS	0.0461 \pm 0.0014
Remove RRWP encoding	0.0797 \pm 0.0040
RRWP encoding \rightarrow relative LapPE*	0.0708 \pm 0.0032
Remove DropKey	0.0549 \pm 0.0125
Remove edge flipping	0.0477 \pm 0.0010
PN-V \rightarrow LN [3]	0.0497 \pm 0.0013
Sum pooling \rightarrow Mean pooling	0.0514 \pm 0.0018

Table 4: Ablation study results on the random regular graph degree r . This table shows the performance of GRASS on ZINC with the corresponding values of r as the mean \pm s.d. over 8 runs. The average variance of model performance due to random rewiring, as well as their sample standard deviations, are also shown. They are measured by evaluating the test set 30 times on each trained model. For comparison, the variance of model performance due to randomness in the training process is 2.03e-6 with the hyperparameters shown in Table 7.

Random Regular Graph Degree r	0	3	6	9	12	15
ZINC MAE \downarrow	0.0495 \pm 0.0016	0.0470 \pm 0.0023	0.0461 \pm 0.0014	0.0473 \pm 0.0015	0.0473 \pm 0.0024	0.0478 \pm 0.0011
Variance in ZINC MAE Due to Random Rewiring	-	6.31e-8 \pm 2.32e-8	1.22e-7 \pm 5.90e-8	1.23e-7 \pm 9.36e-8	1.79e-7 \pm 1.50e-7	1.58e-7 \pm 1.04e-7

D Datasets

Table 5: Statistics of GNN Benchmark Datasets used in section 4, adapted from Rampášek et al. [56].

Dataset	# Graphs	Avg. # Nodes	Avg. # Edges	Task	Metric
ZINC	12000	23.2	24.9	Graph Regression	MAE ↓
MNIST	70000	70.6	564.5	Graph Classif.	Accuracy ↑
CIFAR10	60000	117.6	941.1	Graph Classif.	Accuracy ↑
PATTERN	14000	118.9	3039.3	Node Classif.	Accuracy ↑
CLUSTER	12000	117.2	2150.9	Node Classif.	Accuracy ↑

Table 6: Statistics of LRGB datasets used in section 4, adapted from Dwivedi et al. [24].

Dataset	# Graphs	Avg. # Nodes	Avg. # Edges	Avg. Short. Path	Avg. Diameter	Task	Metric
Peptides-func	15535	150.94	307.30	20.89 ± 9.79	56.99 ± 28.72	Graph Classif.	AP ↑
Peptides-struct	15535	150.94	307.30	20.89 ± 9.79	56.99 ± 28.72	Graph Regression	MAE ↓
PascalVOC-SP	11355	479.40	2710.48	10.74 ± 0.51	27.62 ± 2.13	Node Classif.	Macro F1 ↑

E Hyperparameters

Table 7: Model hyperparameters for experiments on GNN Benchmark Datasets. The results are shown in table 1.

Model	ZINC	MNIST	CIFAR10	PATTERN	CLUSTER
# Parameters	499777	104338	104386	498626	498854
# Attention Layers	49	15	15	53	53
Attention Layer Dim.	32	24	24	32	32
Task Head Hidden Dim.	192	144	144	N/A (Linear)	N/A (Linear)
# Epochs	2000	200	400	500	100
Warmup Epoch Ratio	0.1	0.05	0.1	0.1	0.1
Batch Size	200	200	200	200	200
Initial Learning Rate	1e-7	1e-7	1e-7	1e-7	1e-7
Peak Learning Rate	5e-4	1e-3	1e-3	1e-3	1e-3
Final Learning Rate	1e-7	1e-7	1e-7	3e-4	1e-7
Betas	(0.95, 0.98)	(0.95, 0.98)	(0.95, 0.98)	(0.95, 0.98)	(0.95, 0.98)
Weight Decay Factor	0.3	0.3	0.3	3.0	0.3
Attention DropKey Rate	0.1	0.1	0.1	0.3	0.3
Label Smoothing Factor	N/A (Regression)	0.1	0.1	0.1	0.1
Random Regular Graph Degree	6	3	3	15	15
RRWP Random Walk Length	32	24	24	32	32

Table 8: Model hyperparameters for experiments on LRGB datasets. The results are shown in table 2.

Model	Peptides-func	Peptides-struct	PascalVOC-SP
# Parameters	497866	498155	498133
# Attention Layers	48	48	53
Attention Layer Dim.	32	32	32
Task Head Hidden Dim.	192	192	N/A (Linear)
# Epochs	500	500	600
Warmup Epoch Ratio	0.1	0.1	0.1
Batch Size	200	200	200
Initial Learning Rate	1e-7	1e-7	1e-7
Peak Learning Rate	1e-3	1e-3	1e-3
Final Learning Rate	1e-7	1e-7	1e-7
Betas	(0.95, 0.98)	(0.95, 0.98)	(0.95, 0.98)
Weight Decay Factor	3.0	3.0	1.0
Attention DropKey Rate	0.1	0.1	0.1
Label Smoothing Factor	0.1	N/A (Regression)	0.1
Random Regular Graph Degree	6	6	3
RRWP Random Walk Length	32	32	16

F Computational Performance

Table 9: Computational performance of GRASS on GNN Benchmark Datasets. Training time per epoch is the wall-clock time taken to complete a single training epoch, shown as the mean \pm s.d. over all epochs of a single run. Preprocessing time is the wall-clock time taken to load, preprocess, and store the whole dataset prior to training, shown as the mean \pm s.d. over 4 runs. Specifications of the hardware used to run these experiments are also shown.

Dataset	ZINC	MNIST	CIFAR10	PATTERN	CLUSTER
Training Time per Epoch (s)	2.71 ± 0.13	11.41 ± 0.15	13.08 ± 0.10	150.30 ± 0.17	122.31 ± 0.08
Preprocessing Time (s)	28.35 ± 0.19	74.12 ± 0.44	139.50 ± 6.55	33.08 ± 0.40	27.06 ± 0.10
Model Compilation	Yes			No	
Activation Checkpointing	No			Yes	
GPU	NVIDIA GeForce RTX 4090				
VRAM	24GB				
CPU	AMD Ryzen 9 7950X				
RAM	128GB				

Table 10: Computational performance of GRASS on LRGB datasets. The definitions of these statistics and the procedure of measuring them are identical to that described in Table 9.

Dataset	Peptides-func	Peptides-struct	PascalVOC-SP
Training Time per Epoch (s)	10.44 ± 0.10	10.21 ± 0.09	21.56 ± 0.10
Preprocessing Time (s)	69.78 ± 4.09	69.81 ± 2.18	181.28 ± 1.33
Model Compilation	Yes		
Activation Checkpointing	No		
GPU	NVIDIA GeForce RTX 4090		NVIDIA RTX A6000 Ada
VRAM	24GB		48GB
CPU	AMD Ryzen 9 7950X		
RAM	128GB		